



## Electrochemical and AC Conductivity Studies of PVA based Gel Polymer Electrolytes for Silver Ion Batteries

V. PARTHIBAN<sup>1</sup>, G. SUNITA SUNDARI<sup>1,\*</sup>, C.V.S. BRAHMANANDA RAO<sup>2</sup> and HARIKRISHNA EROTHU<sup>3,4</sup>

<sup>1</sup>Department of Physics, Koneru Lakshmaiah Education Foundation, Vaddeswaram-522502, India

<sup>2</sup>Homi Bhabha National Institute, Indira Gandhi Centre for Atomic Research, Kalpakkam-603102, India

<sup>3</sup>Centre for Advanced Energy Studies (CAES), Koneru Lakshmaiah Education Foundation, Vaddeswaram-522502, India

<sup>4</sup>Department of Chemistry, Koneru Lakshmaiah Education Foundation, Vaddeswaram-522502, India

\*Corresponding author: E-mail: [gunturisunita@kluniversity.in](mailto:gunturisunita@kluniversity.in)

Received: 29 October 2021;

Accepted: 16 March 2022;

Published online: 20 April 2022;

AJC-20787

An effort has been made to synthesize PVA based gel polymer electrolyte films by means of solution casting technique doped with silver ion in different concentration of polymer and salt (80:20, 70:30 and 60:40 wt.%). The resulting PVA and CH<sub>3</sub>COOAg gel polymer electrolyte (GPE) material came to be analyzed through various characterization methods for instance XRD, FTIR and UV-Vis spectrophotometry. The analysis of FTIR and XRD confirmed the polymer and salt complexation. The ionic conductivity for prepared GPE was evaluated by means of AC impedance studies at room temperature. The highest value of ionic conductivity found for PVA: CH<sub>3</sub>COOAg (30 wt.%) system was found to be  $1.422 \times 10^{-5} \text{ S cm}^{-1}$ . The optical and cyclic voltammetric analysis have been examined and excellent cyclic, reversible performance was observed for the electrolyte PVA:CH<sub>3</sub>COOAg (70:30 wt.%) up to 10 cycles.

**Keywords:** Gel polymer electrolyte films, UV-visible spectroscopy, Ionic conductivity, Cyclic voltammetry.

### INTRODUCTION

In recent times, electrochemical energy storing appliances are playing a vital part in the technological applications in electrical communications, industrial controls, electric transport, spaceships, laboratory instruments and some technological devices like computer, *etc.* Besides, they have stubborn requirements in the transportable electronic market like remote controls, pacemakers, toys and in solar cell. In these promising technologies they are exceedingly demanded for long lasting performance, environmentally friendly, less expensive, consistent rechargeable batteries with precise power and energy [1]. Such kind of power was acquired in liquid type electrolytes, which is because of the excellent movement of charge carriers. However there are some drawbacks that is need to rectify in liquid electrolyte like leakage of electrolyte from battery, corrosion of electrode due to reaction with electrode and electrolyte, unstable electrochemical stability, *etc.* so the solid based polymer electrolytes are studied to overcome these defects in the last decades [2]. When it comes to solid polymer electrolyte, it

acquired some excellent advantages like fine mechanical strength of the material, thermal stability which is stable in high temperature and high ionic conductivity of electrolyte. These properties gives interest for many researchers has shifted near the credentials and expansion of solid polymer electrolytes in most advantageous applications such as memory back up in computers, smart windows, traction of electric vehicle, fuel cells, photovoltaic cells and space some power applications, *etc.* [3]. The solid polymer electrolyte is supposed to hold fine mechanical strength throughout manufacturing cell assembly, which acquire structurally stable and leakage of the material will be avoided from cell container [4-6].

To integrate this permanence gel polymer electrolytes (GPE) is particularly a most capable ways, which hold consistent solid properties and also a distributive fluid properties [7,8], therefore these films exhibit high ionic conductivity good mechanical strength as required for device application in rechargeable batteries, fuel cell, sensors, super capacitors, and solar power systems [9,10]. Various GPEs using lithium, sodium, potassium, *etc.* as a salt in battery system are available in the

literature but lithium-based batteries possess some safety limitations [11,12].

In 1924, Hermann & Haehnel first synthesized PVA by saponifying poly (vinyl ester) with sodium hydroxide. It is semi-crystalline biodegradable polymer, soluble in water, odourless and colourless [13]. The varying semi-crystalline to amorphous property of the polymer can be done by using suitable salts, nanofiller, plasticizer or blending polymer host [14]. PVA is a polar substance with many hydroxyl groups and tend to form a inter and intramolecular hydrogen bonds so it has localized stability in the polymer system [13,15,16], which are used in many applications. Many researchers have reported and analyzed several combinations with PVA-GPE films based on lithium, sodium, potassium, *etc.* but very little data on silver salts.

In this work, silver salt is used as alternative to lithium, sodium, *etc.* as it is less expensive, non-toxic and easy to handle in open atmosphere. In the middle of the assorted methods to bring into being good conductivity of ions, suppleness, durability and amorphous property, Polyvinyl alcohol (PVA) based GPE was prepared in the present work, which was the mainly capable and viable approach. The current work is based on PVA based GPE with the complexation of silver acetate and solvent as water using solution casting technique. The function of interface between polymer and silver salt on conductivity of ions and GPEs structural phase were discussed using FTIR, XRD, AC ionic conductivity and optical studies. The GPE has maximum conductivity was analyzed with cyclic voltammetric (CV) and the results of the analysis were also discussed.

## EXPERIMENTAL

Polyvinyl alcohol (PVA) with standard molecular weight 85,000-1,24,000 g/mol (Sigma-Aldrich, USA), silver acetate with molecular weight 166.91 g/mol (Sigma-Aldrich, USA) and deionized water were used in synthesis. The PVA based gel polymer electrolytes were prepared with silver acetate in various concentrations *e.g.* 80:20, 70:30 and 60:40 ratios through solvent casting method through deionized water used as a solvent. The mixed solution was blended up to 48 h at ambient temperature to form a homogeneous mixture. The mixture was decanted into a polypropylene dish and allows to disperse at ambient temperature to eradicate the solvent traces and under vacuum drying for 24 h at 65 °C. Hence, gel polymer electrolyte thin films were obtained and then those films are preserved inside a desiccator.

**Characterization:** The synthesized GPE materials were investigated through FTIR, XRD and UV-Vis spectrophotometry. The XRD studies were accomplished using X-Ray diffraction Rigaku Miniflex 600 with  $\text{CuK}\alpha$  radiation ( $\lambda = 1.54182 \text{ \AA}$ ) with the range of angle  $2\theta = 10\text{-}90^\circ$  and the scanning rate is  $10^\circ$  per min at room temperature. FTIR studies carried out by using FT-IR spectrophotometer CDTL-lab4-EQP-006 in the wave number range are  $4000\text{-}400 \text{ cm}^{-1}$  at room temperature. The UV-visible studies carried out using JASCO V-670 spectrophotometer with the wavenumber range between  $200\text{-}800 \text{ nm}$  optical band gap measured. The impedance analysis

and electrochemical studies were carried out by using PARSTAT PMC 2000A at ambient temperature.

## RESULTS AND DISCUSSION

**XRD studies:** XRD is used to find complete structure of GPE films. The crystalline ones show well demarcated peaks and the amorphous possess broad peaks. Fig. 1 shows (a) non-doped PVA and PVA: $\text{CH}_3\text{COOAg}$ ; (b) (80:20); (c) (70:30) and (d) (60:40) in pure PVA sample at  $20.9^\circ$  contains a sharp peak confirms semi-crystalline character of the material. Same observation was found, when PVA is doped with silver acetate of different wt.% ratios (80:20, 70:30 and 60:40). It is observed that when the concentration of the salt getting rised the sharp intensity peak reduces suggesting semi-crystalline or amorphous nature of the sample. No sharp peak was observed, indicating that dominate polymer is amorphous phase in nature [11]. Similar result was also reported in PVA +  $\text{KMnO}_4$  solid polymer electrolytes [17]. By using Bragg's law, inter planar distance and inter chain interaction were calculated using the following eqns.:

$$D = \frac{\lambda}{2 \sin \theta} \quad (1)$$

where  $\lambda$  is the wavelength and  $\theta$  is the angle of diffraction.

$$R = \frac{7}{2\pi} \times \frac{\lambda}{2 \sin \theta} \quad (2)$$

where R represents length of inter chain,  $\lambda$  denotes the wavelength and  $\theta$  denotes the scattering angle. It is observed that with the decrease of polymer concentration the separation in the inter-chain length and planar distance rises steadily confirmed that the GPE films are semi-crystalline in nature (Table-1). Finally, the broad peak was observed at  $19.5^\circ$  for PVA: $\text{CH}_3\text{COOAg}$  (70:30) GPE film, which is ascribed to amorphous property of the material.

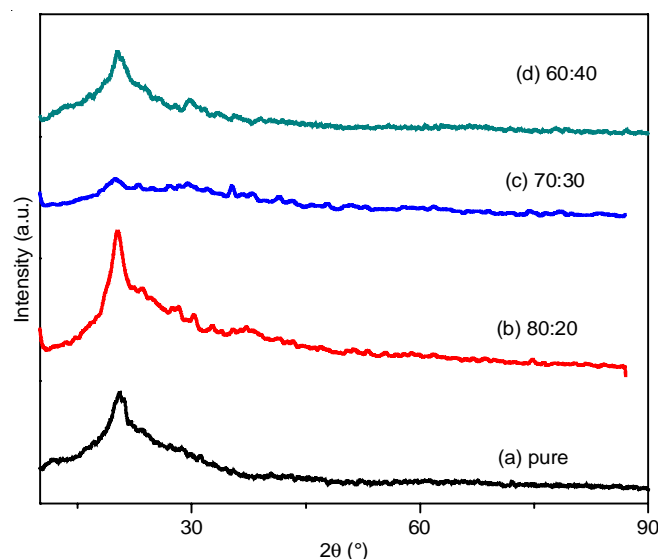


Fig. 1. XRD pattern of (a) PVA (100:00 and PVA: $\text{CH}_3\text{COOAg}$ , (b) (80:20), (c) (70:30) and (d) (60:40)

TABLE-1  
SEPARATION OF INTER CHAIN LENGTH AND  
INTER PLANAR DISTANCE OF PREPARED GPE

PVA: CH <sub>3</sub> COOAg	2θ (°)	Inter chain separation R = 7/2πλ/2sin θ	Inter planar distance d = λ/2sin θ
100:0	20.50	2.453	2.2010
80:20	20.28	2.478	2.2240
70:30	19.84	2.532	2.2714
60:40	20.30	2.476	2.2210

**FTIR studies:** Fig. 2 shows the spectra of PVA (100:00) material complex formation with CH<sub>3</sub>COOAg in dissimilar wt.% ratios (80:20, 70:30 and 60:40). In the stretching of O-H group of PVA (100:00) at 3590 cm<sup>-1</sup> it can be shifted to 2595, 3100 and 3285 cm<sup>-1</sup>, respectively in the PVA+CH<sub>3</sub>COOAg with different ratios (80:20, 70:30 and 60:40). In C-H stretching vibrations of pure PVA was observed at 2880 cm<sup>-1</sup> is shifted to 2925, 2940 and 2985 cm<sup>-1</sup>, respectively in PVA+CH<sub>3</sub>COOAg (80:20, 70:30 and 60:40) with different ratios. The C=O stretching vibrations was absent in pure PVA film is occur at 1710, 1725 and 1730 cm<sup>-1</sup>, respectively in the PVA+CH<sub>3</sub>COOAg with different ratios (80:20, 70:30 and 60:40). Similarly, the C-H bending vibrations at 1395 cm<sup>-1</sup> for PVA (100:00) is shifted to 1410, 1425, 1440 cm<sup>-1</sup>, respectively in PVA+CH<sub>3</sub>COOAg (80:20, 70:30 and 60:40) with different ratios. The C-O stretching vibration was noticed at 1150 cm<sup>-1</sup>, which is shifted to 1210, 1240 and 1265 cm<sup>-1</sup>, respectively in PVA+CH<sub>3</sub>COOAg (80:20, 70:30 and 60:40) with different ratios.

From Table-2, the shift of absorption peaks were observed in PVA:CH<sub>3</sub>COOAg GPE films clearly indicating confirmation of complexation between polymer and salt.

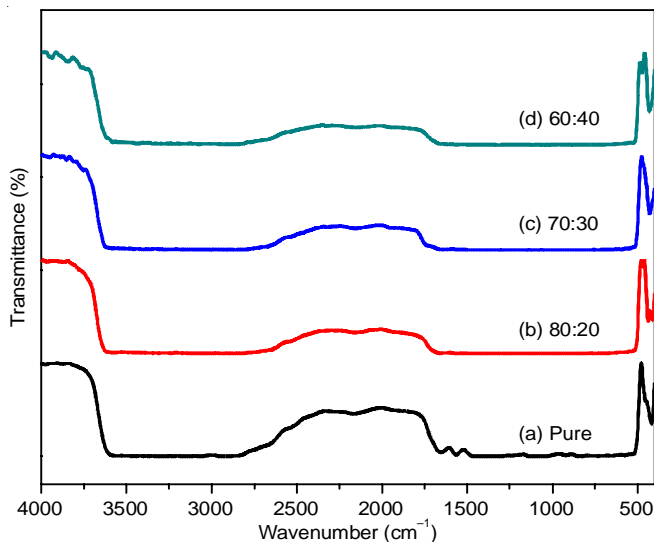


Fig. 2. FTIR spectral analysis for (a) PVA (100:00) and PVA:CH<sub>3</sub>COOAg, (b) (80:20), (c) (70:30) and (d) (60:40)

TABLE-2  
VIBRATIONAL MODES OF FTIR (cm<sup>-1</sup>) SPECTRUM

Mode of vibrations	Pure PVA	PVA:CH <sub>3</sub> COOAg (80:20)	PVA:CH <sub>3</sub> COOAg (70:30)	PVA:CH <sub>3</sub> COOAg (60:40)
O-H bond stretch	3590	2595	3100	3285
C-H bond stretch	2880	2925	2940	2985
C=O bond stretch	Absent	1710	1725	1730
C-O bond stretch	1150	1210	1240	1265
C-H bond bend	1395	1410	1425	1440

**UV-visible analysis:** The UV-visible spectrophotometric studies discuss about the optical absorption of PVA GPE films in the wavelength range of 200-800 nm. In this spectrum (Fig. 3), there is no absorption peak in the range 200-700nm for pure PVA. A broad absorption peak was observed at 423 nm while adding salt with different wt.% ratios.

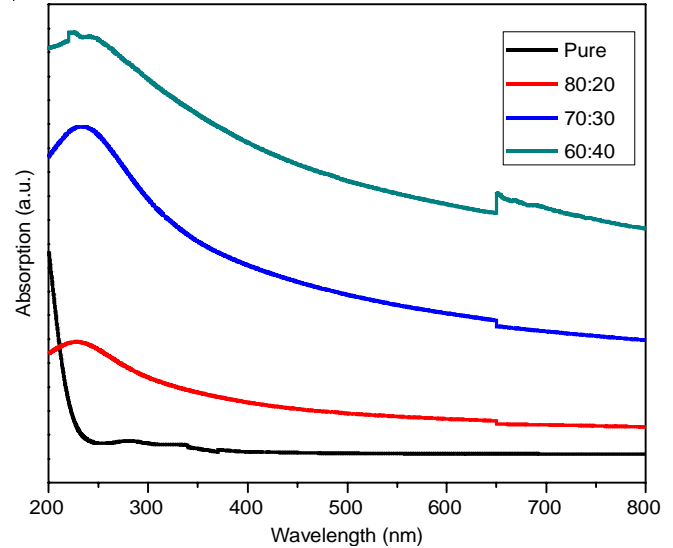


Fig 3. UV-visible spectra of synthesized GPEs with different wt% ratios

**Optical absorption studies:** From these studies, it is found the band structure of the GPE films. The determination of band edge or absorption edge by the transition due to absorption of strong short wavelength and the absorption of weak long wavelength GPE and it is accustomed to find out energy gap. Absorption coefficient ( $\alpha$ ) can be evaluated by the following eqn.:

$$I = I_0 \exp(-\alpha x) \quad (3)$$

Hence,

$$\alpha = \frac{2.303}{x} \log \left( \frac{I}{I_0} \right) = \left( \frac{2.303}{x} \right) A \quad (4)$$

If the maximum level in the valence band and minimum level in the conduction band lies in same line and if they have same k values and therefore satisfies the conservation of energy and momentum are defined as direct band gap, and if the maximum level of valence band and minimum level of conduction band doesn't lie in the same line, then k is different and hence energy and conduction momentum are not conserved which is termed as indirect band gap [18].

To calculate absorption coefficient ( $\alpha$ ), direct  $(\alpha h\nu)^2$  and indirect energy band gap  $(\alpha h\nu)^{1/2}$  graphs had been plotted with

respect to energy of incident photon ( $h\nu$ ) are shown in Figs. 4-6, respectively. Based on the incident photon energy ( $h\nu$ ), direct energy band gap exists and absorption coefficient is specified by

$$\alpha h\nu = C(h\nu - E_g)^{1/2} \quad (5)$$

where  $E_g$  defines the energy band gap,  $C$  represents constant which is based on the sample structure,  $\alpha$  represents absorption coefficient and  $h$  mentions the Planck's constant.

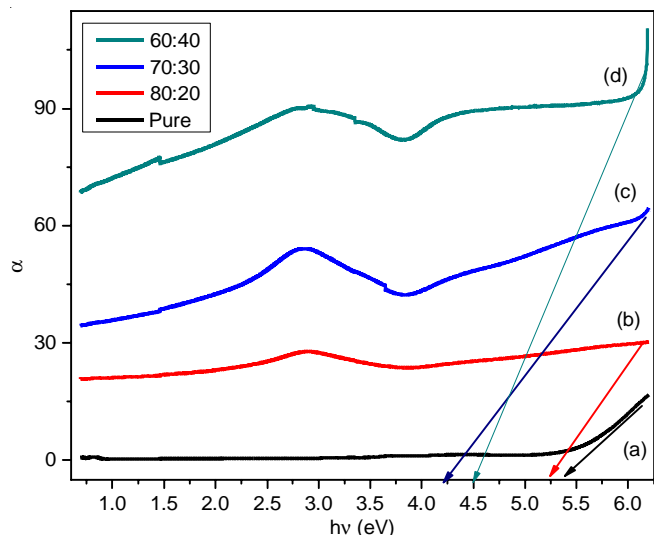


Fig. 4. Graph plotted between photon energy in X-axis and absorption coefficient on Y-axis (a) PVA (100:00) PVA:CH<sub>3</sub>COOAg, (b) (80:20), (c) (70:30) and (d) (60:40)

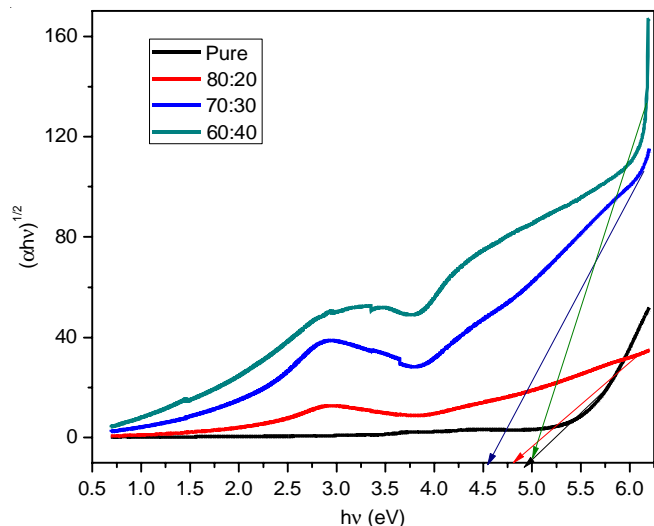


Fig. 5. Indirect band gap vs. photon energy ( $h\nu$ ) plot for (a) PVA(100:00) and PVA:CH<sub>3</sub>COOAg, (b) (80:20), (c) (70:30) and (d) (60:40)

The values regarding direct energy band gap perhaps acquired plotting of  $(\alpha h\nu)^2$  versus  $h\nu$  (photon energy) are shown in Table-3. It is observed that the activation energy decreases, since incorporation of small amount of doping helps in the charge transfer in the complex and hence an increase of ion conductivity is observed (Fig. 6). The direct and indirect energy gap values are changing from higher to lesser values when doping with silver acetate salt in different ratios from

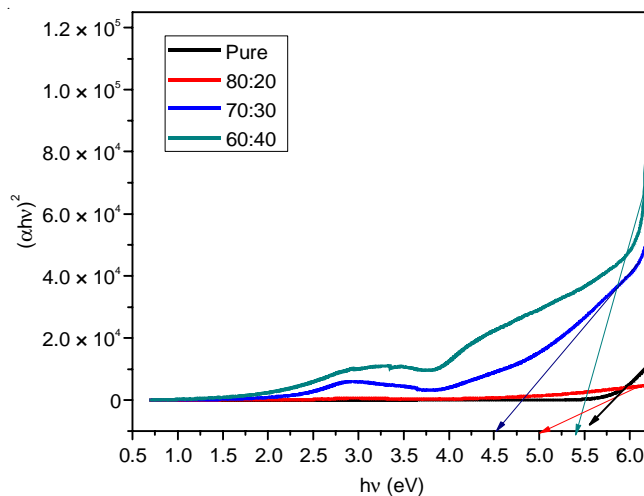


Fig. 6. Direct band gap vs. photon energy ( $h\nu$ ) plot of (a) PVA (100:00) and PVA:CH<sub>3</sub>COOAg, (b) (80:20), (c) (70:30) and (d) (60:40)

Films	Optical band gap		Adsorption edge
	Direct	Indirect	
PVA (100:00)	5.6	5.1	5.4
PVA:CH <sub>3</sub> COOAg (80:20)	5.0	4.9	5.2
PVA:CH <sub>3</sub> COOAg (70:30)	4.5	4.6	4.2
PVA:CH <sub>3</sub> COOAg (60:40)	5.4	4.8	4.5

the above result lowest direct and indirect band observed in PVA:CH<sub>3</sub>COOAg (70:30) GPE film. This compositional ratio could improve the ionic conductivity.

### Conductivity studies

**Electro impedance spectroscopy (EIS):** The galvanostatic EIS exhibits a plot between real part versus (80:20, 70:30 and 60:40) of PVA with CH<sub>3</sub>COOAg of GPE were analyzed using electro impedance spectroscopy (EIS) method. The GPE films were sandwiched between coin type silver blocking electrodes (silver/GPE/silver). The conductivity can be measured in the frequency range 1000 Hz-1 MHz, 1000 Hz-5 MHz at room temperature. The high frequency region in the Nyquist plot (Cole-Cole) usually denotes a semi-circular arc. The ionic conductivity in the gel polymer electrolytes are related upon the mobility of ion and the number of effective carrier ions. The numbers of effective carrier ions are related to concentration of diffused ions. The mobility of ion in GPE films can form by means of the fragment mobility in the polymer chains [19]. The ionic conductivity was calculated by using eqn. 6:

$$\alpha = \frac{L}{R_b \times A} \quad (6)$$

where  $L$  denotes the sample breadth of the prepared GPE material;  $A$  represents the area measured in blocking electrode and  $R_b$  is the bulk resistance found in the Nyquist plot of GPE films [20].

The ionic conductivity of GPE films for different wt.% ratios (80:20, 70:30 and 60:40) are reported. The pure PVA ionic conductivity was found to be  $1.87 \times 10^{-10}$  S cm<sup>-1</sup> at the



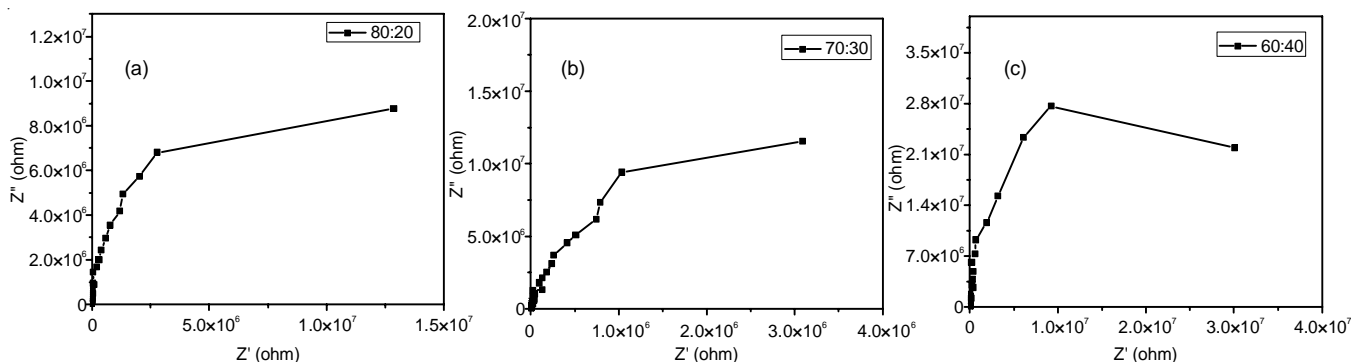


Fig. 7. Cole-Cole plots of gel electrolyte films with different w% ratio of (a) 80:20, (b) 70:30, (c) 60:40

ambient temperature. Increased in the conductivity of the GPE was observed when the ratio of salt content increases. The ionic conductivity values are shown in Table-4. The highest value of ionic conductivity was  $1.422 \times 10^{-5} \text{ S cm}^{-1}$  obtained to PVA:CH<sub>3</sub>COOAg 70:30 wt.% ratio, which is compared with literature data [21].

Films	Conductivity at room temperature
PVA (100:00)	$1.87 \times 10^{-10} \text{ S cm}^{-1}$
PVA + CH <sub>3</sub> COOAg (80:20)	$2.55 \times 10^{-6} \text{ S cm}^{-1}$
PVA + CH <sub>3</sub> COOAg (70:30)	$1.442 \times 10^{-5} \text{ S cm}^{-1}$
PVA + CH <sub>3</sub> COOAg (60:40)	$1.37 \times 10^{-6} \text{ S cm}^{-1}$

Imaginary part, in this impedance analysis Cole-Cole plots were obtained (Fig. 7), the conductivity was measured with different wt.% ratio.

**DC conductivity studies:** Fig. 8 shows the DC ionic conductivity variations of  $\log \sigma_{DC}$  versus temperature ( $1000/T$ ) in K. The DC conductivity for prepared GPE films were analyzed in the temperature range of 303-333 K. It clearly defines that increasing the temperature and concentration of salt shows rise in conductivity. The DC conductivity can be calculated by using Arrhenius equation:

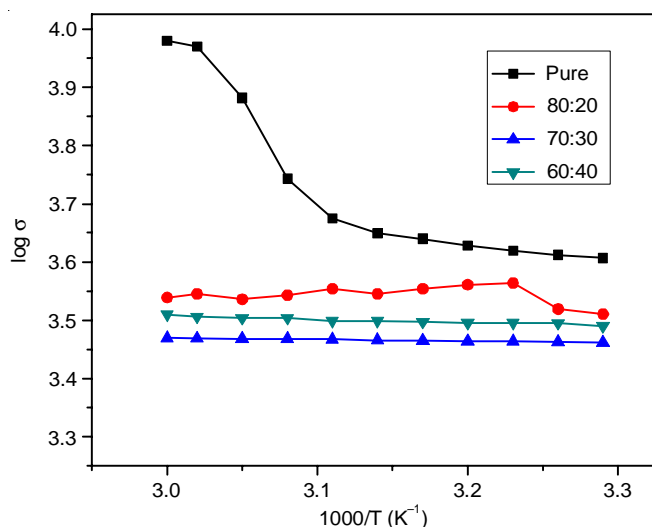


Fig. 8. The d<sub>c</sub> conductivity of (a) PVA (100:00) and PVA:CH<sub>3</sub>COOAg, (b) (80:20), (c) (70:30) and (d) (60:40)

$$\alpha_{dc} = \exp\left(\frac{-E_a}{kT}\right) \quad (7)$$

where  $\sigma_0$  is considered as pre-exponential factor,  $E_a$  be termed as activation energy,  $k$  declares to be Boltzmann constant and  $T$  gives temperature in Kelvin. The DC ionic conductivity were evaluated by the following relation:

$$\alpha_{dc} = \frac{(i \times L)}{(V \times A)} \quad (8)$$

where  $i$  represents the current,  $L$  and  $A$  represents length and area of GPE,  $V$  denotes the applied constant voltage.

Fig. 9 shows that the conductivity has increased two-fold. The conductivity for pure PVA polymer film was  $1.83 \times 10^{-10} \text{ S/cm}$  at room temperature. The rising salt concentration and temperature leads to rise in the conductivity up to 333 K. The activation energy can be derived from the data of salt concentration versus activation energy. The calculated activation energy values are shown in Table-5. The activation energy decreased when the salt concentration increases, the highest conductivity and lowest activation energy was observed in PVA:CH<sub>3</sub>COOAg (70:30) wt.% ratio system.

**Linear sweep voltammetry:** The LSV was operated on the highest conductivity film PVA:CH<sub>3</sub>COOAg (70:30 wt.%) by using a cell containing SS//GPE//silver, where the stainless

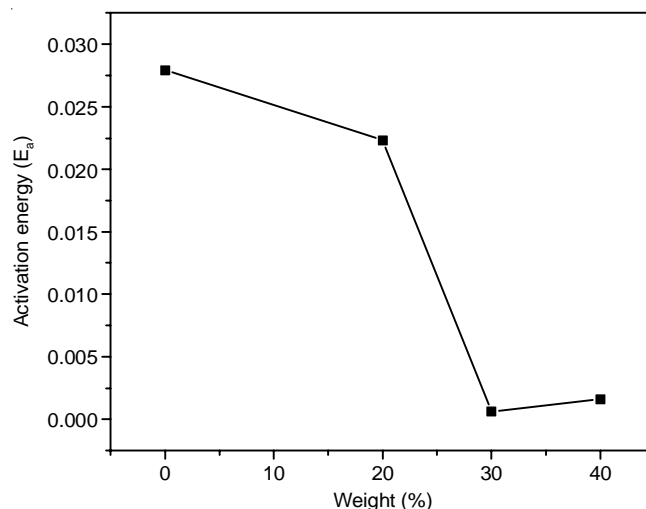


Fig. 9. Variation of activation energy for PVA with CH<sub>3</sub>COOAg different concentration w% ratios

TABLE-5  
ACTIVATION ENERGIES OF PVA WITH  
CH<sub>3</sub>COOAg GEL POLYMER ELECTROLYTES

Films	Activation energy (E <sub>a</sub> )
PVA (100:00)	0.02790300
PVA + CH <sub>3</sub> COOAg (80:20)	0.02233200
PVA + CH <sub>3</sub> COOAg (70:30)	0.00065200
PVA + CH <sub>3</sub> COOAg (60:40)	0.00131308

steel (SS) worked as working electrode and GPE film as counter electrode plus silver metal worked as a reference electrode.

The voltage from 0V has varied to anodic (positive) values with the scan rate 50 mV s<sup>-1</sup> and large current was obtained. Fig. 10 shows result of the voltammogram of these cells and following observations were made as follows:

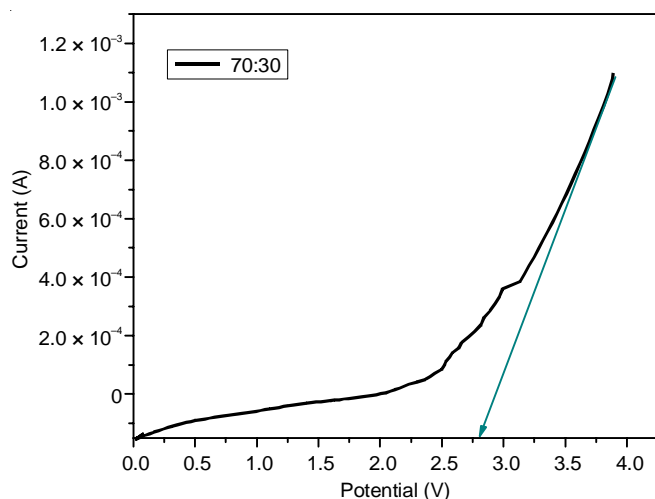


Fig. 10. Linear sweep voltammogram of GPE containing a 30 wt.% of silver acetate scan rate at 50 mV s<sup>-1</sup>

(i) At high voltage range on the potential axis a sudden increase in the current was occurred at definite potential, this is caused by the GPE decomposition at interface of electrode.

(ii) It was measured to be 2.7 V, which indicates electrochemical stability window of GPE films indicating that GPE films has good electrochemical stability (> 2.0 V) for silver cell.

(iii) At lower voltages, the observed current density is due to the combined result of the ionic conductivity of GPE and common boundaries resistance of silver metal or GPE.

**Cyclic voltammetry studies:** The working electrode is cathode, counter electrode is a GPE, and reference is an anode (stainless steel // GPE // silver). The potential from working electrode is increased linearly with respect to time, at the same time the reference electrode uphold constant potential. The purpose of GPE present here is to present ions to electrodes during redox process. As potential decreases, electrode becomes more reducing hence reduction current will increase and when potential increases, electrode becomes more oxidizing hence oxidation current increases [22,23]. Silver ion battery cell system was fabricated and using electrochemical workstation CV and LSV studies were carried out and tested for the rechargeable battery system.

**Cyclic voltammetry:** Fig. 11 shows the cyclic voltammogram of PVA:CH<sub>3</sub>COOAg (70:30 wt.%) polymeric electrolyte

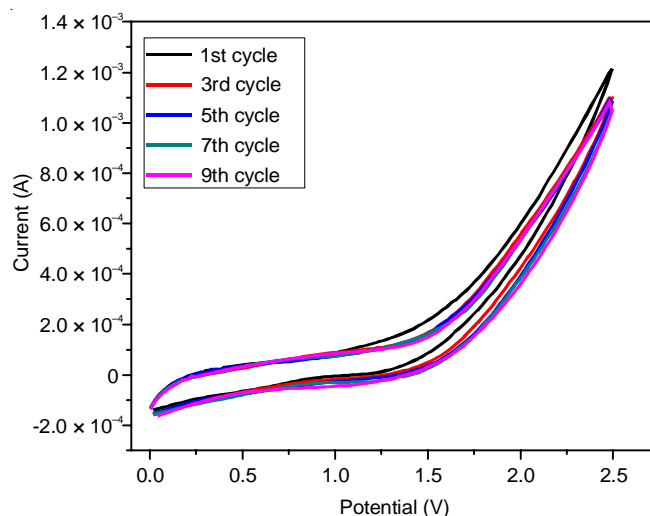


Fig. 11. Cyclic voltammogram of GPE containing a 30 wt.% of silver acetate scan rate at 50 mV s<sup>-1</sup>

films. It has been performed for the silver// GPE//Silver cell system at the scanning speed of 50 mV s<sup>-1</sup> up to 10 cycles to establish that the prepared GPE has an exceptional reversibility.

When the system was tested, it was observed that 2.7 V at scan rate 50 mV s<sup>-1</sup> electrochemical stability was achieved for the GPE materials, exhibiting the excellent electrochemical stability (> 2.0 V) for silver cell.

The electrochemical stability has been observed from 0 to 2.7 V for PVA:CH<sub>3</sub>COOAg (70:30 wt.%) for 1st, 3rd, 5th, 7th and 10th cycle and during initial cycle there was a decrease in current but slowly due to development of passivation layer on the electrode took place therefore stability of the current was observed. The cyclic voltammogram sturdily point out that the GPE with 30% of silver acetate film has excellent reversibility and adequate electrochemical stability for the functioning in the silver ion battery system. The GPE possess good cyclic and reversible property is PVA:CH<sub>3</sub>COOAg (70:30 wt.%) up to 10 cycles.

## Conclusion

A PVA based gel polymer electrolyte (GPE) films were prepared using solution casting technique with silver acetate salt and deionized water as solvent. The XRD and FTIR results show the complexation between polymer and salt. The UV-Visible studies indicated that the optical band gap was reduced when salt concentration increases. AC impedance studies showed the highest conductivity obtained at  $1.422 \times 10^{-5}$  S cm<sup>-1</sup> for PVA:CH<sub>3</sub>COOAg (70:30) at room temperature. The linear sweep voltammetry (LSV) studies concluded that the GPE film has electrochemically stability up to 2.7 V and the cyclic voltammetric (CV) studies showed the fine cyclic and reversible stability attained for PVA:CH<sub>3</sub>COOAg (70:30 wt.%) up to 10 cycles.

## ACKNOWLEDGEMENTS

The authors are thankful to Er. K. Satyanarayana, President of Koneru Lakshmaiah Education Foundation (KLEF) for providing the laboratory facilities and IGCAR/UGC-DAE CSR

Kalpakkam (CSR-KN/CRS-120/2018-19/1058) for funding. Special acknowledgment to Dr. K. Swapna for the UV-Vis spectrophotometry analysis.

### CONFLICT OF INTEREST

The authors declare that there is no conflict of interests regarding the publication of this article.

### REFERENCES

1. K.S. Ngai, S. Ramesh, K. Ramesh and J.C. Juan, *Ionics*, **22**, 1259 (2016); <https://doi.org/10.1007/s11581-016-1756-4>
2. B. Scrosati and C.A. Vincent, *MRS Bull.*, **25**, 28 (2000); <https://doi.org/10.1557/mrs2000.15>
3. S. Kurapati, S.S. Gunturi, K.J. Nadella and H. Erothu, *Polym. Bull.*, **76**, 5463 (2019); <https://doi.org/10.1007/s00289-018-2659-5>
4. R.C. Agrawal and G.P. Pandey, *J. Phys. D Appl. Phys.*, **41**, 223001 (2008); <https://doi.org/10.1088/0022-3727/41/22/223001>
5. S.S. Sekhon, *Bull. Mater. Sci.*, **26**, 321 (2003); <https://doi.org/10.1007/BF02707454>
6. L. Sa'adu, M.A. Hashim, M.B. Baharuddin, *J. Mater. Sci. Res.*, **3**, 48 (2014); <https://doi.org/10.5539/jmsr.v3n4p1>
7. J.E. Weston and B.C.H. Steele, *Solid State Ion.*, **7**, 75 (1982); [https://doi.org/10.1016/0167-2738\(82\)90072-8](https://doi.org/10.1016/0167-2738(82)90072-8)
8. J.R. MacCullum and C.A. Vincent, *Polymer Electrolyte Reviews-1*, Elsevier Applied Science Publishers: London (1987).
9. G. Hirankumar and N. Mehta, *Heliyon*, **4**, e00992 (2018); <https://doi.org/10.1016/j.heliyon.2018.e00992>
10. A.M. Stephan, *Eur. Polym. J.*, **42**, 21 (2006); <https://doi.org/10.1016/j.eurpolymj.2005.09.017>
11. A.R. Polu and R. Kumar, *Int. J. Polym. Mater.*, **62**, 76 (2013); <https://doi.org/10.1080/00914037.2012.664211>
12. M. Marzantowicz, J.R. Dygas and F. Krok, *Electrochim. Acta*, **53**, 7417 (2008); <https://doi.org/10.1016/j.electacta.2007.12.047>
13. M. Aslam, M.A. Kalyar and Z.A. Raza, *J. Polym. Eng. Sci.*, **58**, 2119 (2018); <https://doi.org/10.1002/pen.24855>
14. S. Pokhrel and L.S. Rai, *J. Nepal Chem. Soc.*, **40**, 57 (2019); <https://doi.org/10.3126/jncs.v40i0.27283>
15. S.K.S. Basha, G.S. Sundari and K.V. Kumar, *Mater. Today Proc.*, **3**, 11 (2016); <https://doi.org/10.1016/j.matpr.2016.01.109>
16. K. Sravanthi, G.S. Sundari and H. Erothu, *Optik*, **241**, 166229 (2021); <https://doi.org/10.1016/j.ijleo.2020.166229>
17. O.G. Abdullah, S.B. Aziz and M.A. Rasheed, *Results Phys.*, **6**, 1103 (2016); <https://doi.org/10.1016/j.rinp.2016.11.050>
18. M. Ramaswamy, T. Malayandi, S. Subramanian, J. Srinivasalu, M. Rangaswamy and V. Soundararajan, *Polym. Plast. Technol. Eng.*, **56**, 992 (2017). <https://doi.org/10.1080/03602559.2016.1247280>
19. P. Santhosh, T. Vasudevan, A. Gopalan and K.-P. Lee, *J. Power Sources*, **160**, 609 (2006); <https://doi.org/10.1016/j.jpowsour.2006.01.091>
20. L.-Z. Fan and J. Maier, *Electrochem. Commun.*, **8**, 1753 (2006); <https://doi.org/10.1016/j.elecom.2006.08.017>
21. S. Aziz, R. Abdullah, M. Rasheed and H. Ahmed, *Polymers*, **9**, 338 (2017); <https://doi.org/10.3390/polym9080338>
22. J.E.B. Randles, *Trans. Faraday Soc.*, **44**, 327 (1948); <https://doi.org/10.1039/TF9484400327>
23. X. Huang, Z. Wang, R. Knibbe, B. Luo, S.A. Ahad, D. Sun and L. Wang, *Energy Technol.*, **7**, 1801001 (2019); <https://doi.org/10.1002/ente.201801001>